Five Scales of Airflow Associated with a Series of Downbursts on 16 July 1980

T. THEODORE FUJITA AND ROGER M. WAKIMOTO

The University of Chicago, Chicago, IL 60637

(Manuscript received 5 September 1980, in final form 17 March 1981)

ABSTRACT

A series of destructive windstorms on 16 July 1980 in a 50 km (30 mi) wide zone from Chicago to Detroit was surveyed both from the air and the ground. In spite of the initial suspicion of 10–20 tornadoes in the area, the nature of the windstorms was confirmed to be downbursts and microbursts characterized by multiple scales of airflows with their horizontal dimensions extending tens of meters to hundreds of kilometers.

An attempt was made to estimate the wind speed based on three types of airborne objects: a 180 kg (390 lb) chimney, a 1000 kg (one ton) corn storage bin, and lumber from damaged roofs found inside downburst areas, obtaining the maximum wind speed of 63 ± 10 m s^{-1} (140 ± 25 mph). A total of $500 million damage reported was caused by thunderstorm-induced non-tornadic storms which affected very large areas.

SMS/GOES pictures showed that the parent cloud was oval-shaped with its lifetime in excess of 12 h. The overshooting areas enclosed by the −66°C isotherms shrunk rapidly at the onset of the Chicago-area downbursts, indicating that the downbursts began when overshooting activities subsided. This variation of the overshooting features, however, does not necessarily imply a direct physical link between the collapsing top and the downbursts at the surface. This paper presents cloud-top features and wind effects on the ground with no attempt to relate them on the basis of conceptual models currently available.

1. Introduction

Suckstorff (1938) postulated that precipitation cooling within thunderstorms causes an outflow of cold air which results in strong surface winds. As air traffic increased in the late 1930's, squall-line related accidents occurred in various parts of the world, resulting in the operation of fact-finding projects of thunderstorms and squall-line circulations.

Results of the Japanese Thunderstorm Observation Project by Fujiwara (1943), the U.S. Thunderstorm Project by Byers and Braham (1949), and the German Squall Line Project by Koschmieder (1955) confirmed that most thunderstorms are characterized by downdraft cells during their post-development stages. The fields of divergence induced by downdrafts descending to the ground were estimated by anemometers. In many cases, peak values of the divergence were underestimated as a result of network resolutions. The observational evidence during the 1940's and 1950's led to a presumption that most downdrafts weaken before reaching the ground without inducing violent outflow winds near the ground.

On the other hand, Müldner (1950) found a number of diverging patterns of tree damage left behind by the Nürenberg, Germany thunderstorm of 22 July 1948. The characteristic dimensions of diverging patterns were 3–5 km across. At that time, no one related the localized wind with the foot of a strong downdraft which could spread out violently and result in uprooted trees and damaged houses.

There are numerous reports of uprooted trees in NOAA's *Storm Data* in which types of damaging winds are classified as tornado or straight-line winds. Straight-line winds are assumed to be those which rush out of thunderstorms behind advancing gust fronts which are tens of kilometers in length.

After a meteorological study of the Eastern 66 accident at New York City's JFK Airport, Fujita[1] concluded that a strong downdraft could induce an outburst of damaging wind on or near the ground. He called the foot of such a strong downdraft, including both downflow and outflow, the "downburst."

Definitions of downburst

In 1976 and 1977, the downburst was defined exclusively for aviation purposes. In later years, as the knowledge of the scale and intensity of the phenomenon increased, the term was redefined meteorologically.

[1]Spearhead echo and downburst near the approach end of a John F. Kennedy runway, New York City (printed March 1976 as SMRP Res. Pap. 137, 51 pp.), prepared for airline pilots, presents the definition of "downburst" for aviation. Copies of the paper are available from the author.

0027-0644/81/071438-19$08.75

1) IN AVIATION

A localized, intense downdraft with vertical currents exceeding the vertical speed of an aircraft during its landing and departing operations. The vertical speed is approximately 3.6 m s^{-1} (12 ft s^{-1}) at 91 m (300 ft). Refer to Fujita and Byers (1977) and Fujita and Caracena (1977).

2) IN METEOROLOGY

A strong downdraft which induces an outburst of damaging winds on or near the ground. A small downburst with its horizontal dimensions <4 km is called a microburst. For the initial definition, refer to Fujita.[2]

Fujita and Byers (1977) pointed out that the vertical speed of downbursts is about 10 times the mean downdraft speed estimated from the Thunderstorm Project data. Subsequently, the question may arise as to the ultimate strength of downbursts which can be expressed by (i) the maximum wind speeds, both vertical and horizontal, and (ii) the height above the ground at which the maximum horizontal wind speeds occur.

In answering question (i), Fujita and his collaborators at the University of Chicago have performed aerial surveys of downburst damage. The survey results in Table 1 indicate that the maximum assessed damage in downbursts was F3 with an associated wind speed range of 71–92 m s^{-1}.

2. Five scales of downburst-related damage patterns

Since downbursts were defined in 1976, Fujita and his collaborators made special efforts to fly over areas damaged by severe thunderstorms in search of various scales of wind effects left behind by downbursts.

Subsequent analyses of aerial photographs revealed the existence of multiple scales of damage patterns which are now classified into five scales. The horizontal dimensions of these scales extend from tens of meters to several hundred kilometers.

In order to cover the entire range of downburst-related damage patterns, the terms "masoscale" and "misoscale" (read as mysoscale) were introduced. These new terms and their relationship with the mesoscale are shown in Fig. 1. Each of these scales is divided into ALPHA (larger) and BETA (smaller) scales for subscale identification.[3]

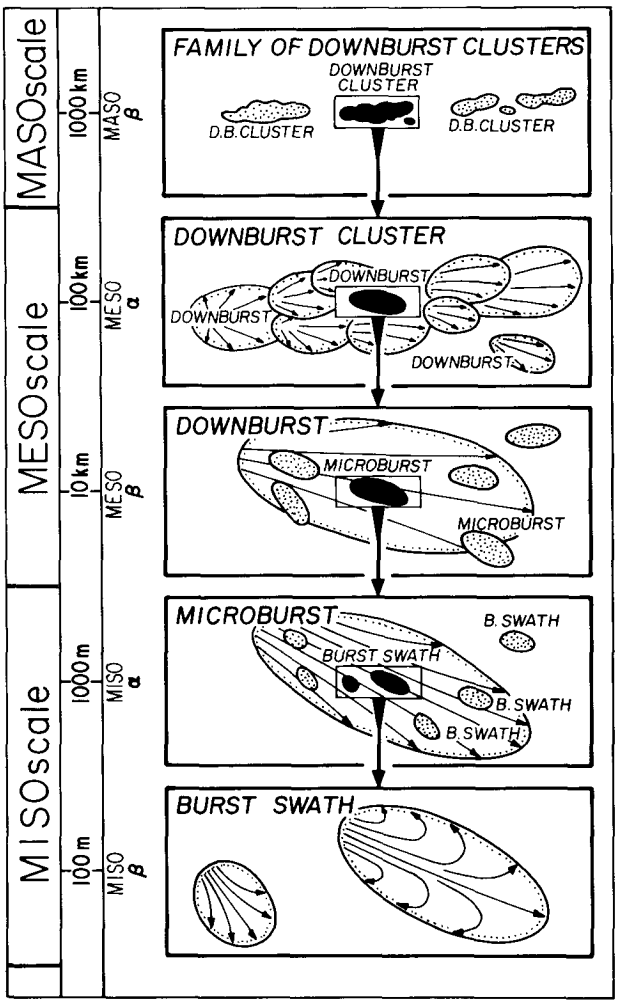

FIG. 1. Five scales of downburst damage patterns. A family of downburst clusters extends several hundred kilometers while a downburst cluster consists of a number of individual downbursts. Microbursts frequently occur without a parent downburst. A burst swath, particularly a long and narrow one, is characterized by damage typical of tornadoes.

[2]Manual of downburst identification for Project NIMROD (printed May 1978 as SMRP Res. Pap. 156, 104 pp.), distributed to all National Weather Service Field Offices, defines microburst as a microscale downburst. Copies of the manual are available from the author.

TABLE 1. Intensity distribution of 24 148 tornadoes (1916–77) and 142 downbursts (1973–77) surveyed with the Fujita (1973) classification scheme.

Storm types	F0	F1	F2	F3	F4	F5
Tornadoes (%)	23	35	29	11	2.8	0.5
Downbursts (%)	47	32	19	1.4	none	none

[3]Horizontal dimensions for dividing maso-, meso- and misoscales in Fig. 1 are chosen to be 400 km and 4 km which are the wavelengths of wavenumbers 100 and 10 000 on the earth's equator, 40 000 km long. The ALPHA and BETA subscales are divided by 4000 km, 40 km and 400 m lengths, corresponding to wavenumbers 10, 1000 and 10 000. For definition and further information of this scale, refer to "Tornadoes and downbursts in the context of generalized planetary scales" by Fujita to be published in the "Special Mesoscale Issue" of *J. Atmos. Sci.* (1981).

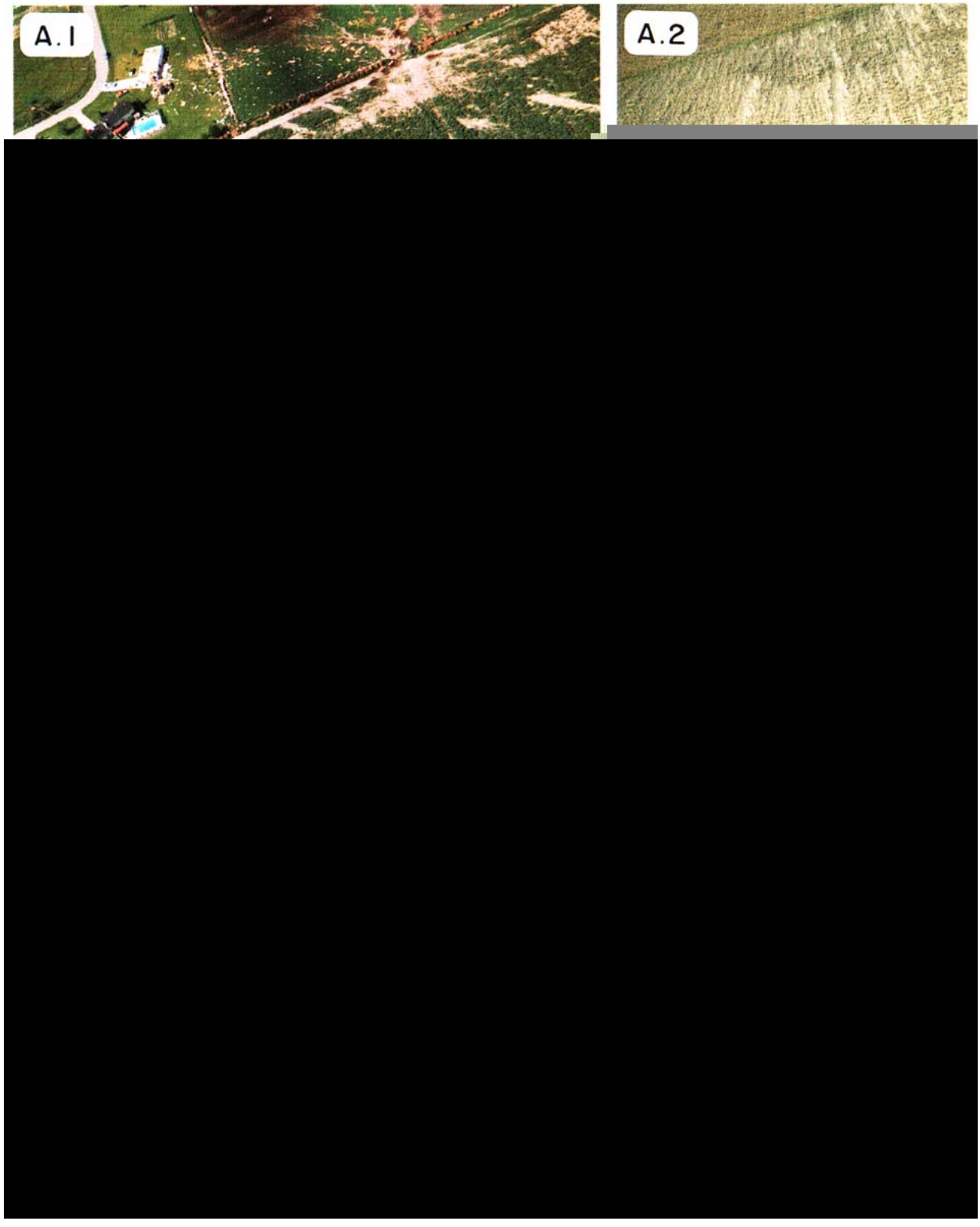

FIG. 2. Aerial photographs showing the wind effects of microbursts and burst swaths. (A1) Battle Creek, Michigan microburst 16 July 1980; (A2) Danville, Illinois microburst 30 September 1977; (A3) Grand Haven, Michigan burst swath 10 August 1979; (A4) Battle Creek, Michigan burst swath; (A5) Alamo, Indiana downflow deflected by a slanted roof 30 September 1977; (A6) Danville, Illinois burst swath 30 September 1977.

It has been found that the majority of downbursts identified through aerial photogrammetric mapping falls into the meso-BETA and miso-ALPHA categories with their dimensions extending between 400 m and 40 km. Misoscale downbursts (called "microbursts") are often embedded inside the meso-BETA scale downburst. Also found frequently inside a microburst are small swaths of diverging winds, called "burst swaths."

Fig. 2 with views A1–A6, shows examples of wind effects in microbursts and burst swaths photographed from 150 to 600 m (500 to 2000 ft) above the ground. A1 shows numerous pieces of roofing materials blown into the cornfield by a microburst, to be discussed in this paper. Corn crops in A2 were blown down by microburst winds in Illinois.

Burst swaths, often embedded inside a microburst, affect relatively small areas, but their wind effects are severe and concentrated. A3 shows numerous trees in a forest blown down by a burst swath in Michigan. A roof of a house near the lower left corner of A4 landed on the other side of a house across the road carrying with it an 180 kg (360 lb) chimney. This event is discussed in this paper.

A5 is a view from 300 m above the cornfield showing the slanted downflow deflected by the roof of an outbuilding in a farm near Alamo, Indiana. The roof was slightly damaged while the cornstalks were blown down by the deflected high winds. A trailer in A6 in a burst swath was blown over a propane tank and disintegrated upon impact in the cornfield. There were no visible signs of a tornado in the damage patterns.

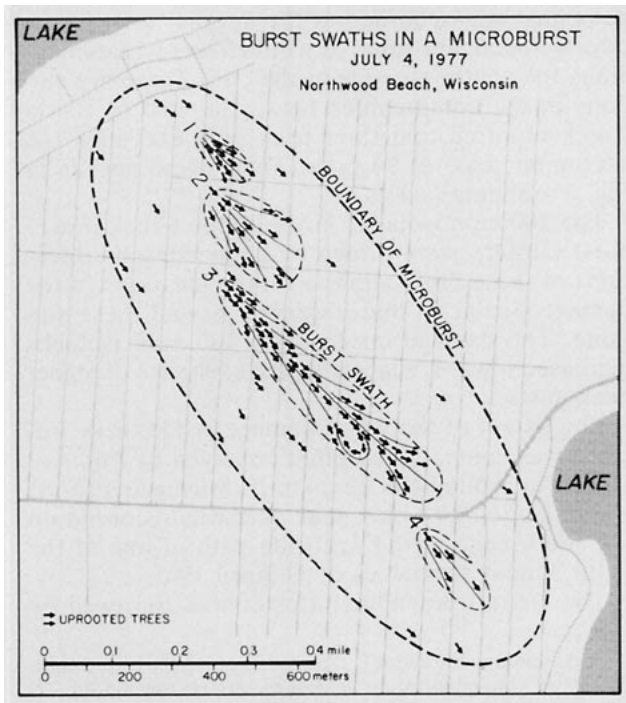

FIG. 3. Four burst swaths mapped inside a northern Wisconsin microburst. Northwood Beach, located between two lakes, is flat and uniformly covered with pine trees, 7–10 m tall. The tree-fall pattern in each swath is highly divergent. Swath 3 showed an anticyclonic eddy on its forward right side.

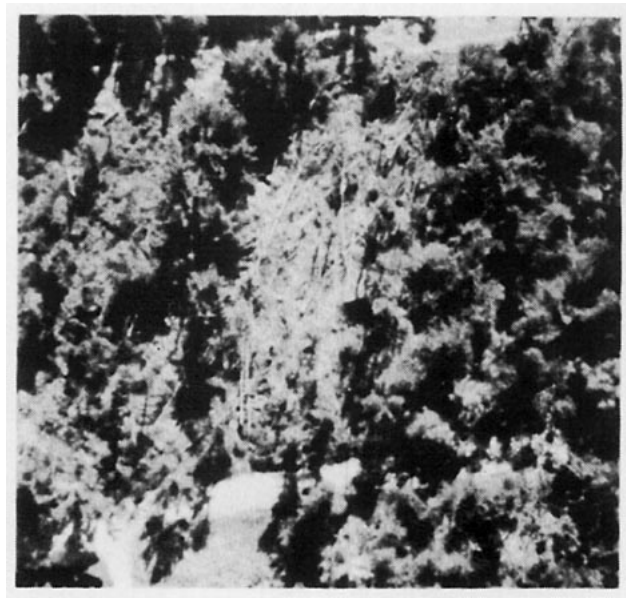

FIG. 4. An aerial photo of burst swath No. 3 in Fig. 3. The width of the 100–150 mph (45–67 m s^{-1}) wind swath was 40 to 70 m. This type of damage has often been reported as tornado damage. (Photo by Fujita).

Based on the aerial surveys of downburst damage, including the 16 July 1980 case reported in this paper, damage patterns in five scales were defined as follows:

1) Family of downburst clusters (maso-BETA scale): A series of downburst clusters produced by one storm system as it travels hundreds of kilometers (Fig. 1).

2) Downburst cluster (meso-ALPHA scale): An overall area of wind damage consisting of two or more downbursts (Fig. 1).

3) Downburst (meso-BETA scale): A strong downdraft which induces an outburst of damaging winds over a meso-BETA-scale area. Damaging winds, either straight or curved, are highly divergent. One or more microbursts can be found within a downburst (Fig. 1).

4) Microburst (miso-ALPHA scale): A strong downdraft which induces an outburst of damaging winds over a miso-ALPHA-scale area. The life of a microburst is <20 min, causing potential difficulties in aircraft operations at low levels, if not detected in time for an alert (Figs. 1 and 2).

5) Burst swath (miso-BETA scale): A swath of extreme wind occurring inside a downburst or microburst. A long and narrow burst swath often resembles a path of a tornado (Figs. 1, 2, 3, and 4).

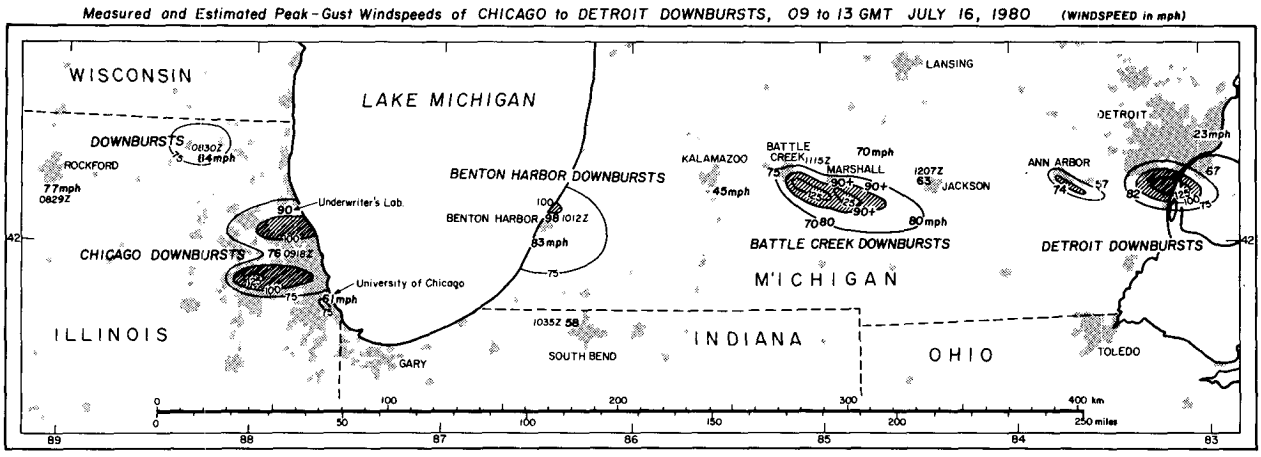

FIG. 5. Chicago-to-Detroit downbursts of 16 July 1980, consisting of a family of four downburst clusters. Survey credit: Chicago area, Levine, Fujita and Duval; Benton Harbor and Detroit areas, Snider; Battle Creek area, Wakimoto, Fujita, Abbey and Jacobson.

The 16 July 1980 storm was rather unusual, because we were able to confirm all of the five scales of damage patterns defined above. The objectives of this paper are to describe these scales of motion along with the estimates of approximate wind speeds required to cause the observed wind effects.

3. Four downburst clusters of 16 July 1980

The Chicago to Detroit downbursts (0830–1300 GMT) which caused $500 million of damage were preceded by earlier downbursts (0100–0400 GMT) near Eau Claire, Wisconsin, which left $150 million of damage. The parent clouds of these storms were two different nephsystems identifiable in SMS/GOES infrared imagery.

A series of downbursts began at 0830 GMT (0330 CDT) northwest of Chicago near the Wisconsin border where an anemometer reading of 84 mph peak gust was made. Scattered power failures were reported in the same area (see Fig. 5).

At about 1300 GMT the last downbursts left the Detroit, Michigan area moving into Ontario, Canada. Most of the intense downbursts, during the 4.5 morning hours, occurred in four separate groups of downburst clusters.

A downburst cluster, analogous to a cloud cluster in the tropics, consists of several downbursts of various dimensions. Four clusters in Fig. 5 are identified as the Chicago downburst cluster, the Benton Harbor downburst cluster, the Battle Creek downburst cluster, and the Detroit downburst cluster. These clusters form a "family of downburst clusters" located inside a band extending from Chicago, Illinois to Detroit, Michigan.

The damage between these downburst clusters was insignificant. For instance, there was little or no damage in the far west suburbs of Chicago. Wind damage increased rapidly in the near west suburbs, which were initially attributed to tornado damage. Of course, there is no way of estimating what happened over the lake. Wind effects decreased from east of Benton Harbor to Kalamazoo, Michigan.

The Kalamazoo area was free from damage, where a peak gust of only 45 mph (20 m s^{-1})[4] was measured at the city airport. The wind effects increased again toward Battle Creek, where a 75 mph peak gust was recorded at the airport, west of the city. A significant surge of wind effects was evident along the southeast edge of the city. Three fire stations in the communities far to the east of Battle Creek reported that their peak gust exceeded the maximum scale of 90 mph. These wind speeds in Fig. 5 are identified as 90+.

The 100 mph isotachs in the Battle Creek downburst clusters were drawn by connecting the locations of these fire stations with the locations of the damage similar to that observed around these stations. The damage inside these 100 mph isotachs increased inward, suggesting the existence of higher peak gusts.

The extent of the worst damage inside these isotachs was comparable to that observed by Fujita *et al.* (1970) around the Tecumseh, Michigan airport, where a 151 mph[5] plus peak gust was recorded on the south edge of a 4 km wide path of one of the Palm Sunday tornadoes of 11 April 1965.

The Detroit downburst cluster was surveyed by

[4]Wind speed measured and reported in miles per hour (mph). The speed converted to the nearest meters per second (m s^{-1}) is given in parentheses in Sections 3–5.

[5]The anemometer survived, recording the wind direction and speed during the tornado which passed 2 km north; recording pen hit the upper limit of the deflection at 151 mph; observed from the air some roof damage near the anemometer; unroofed houses and uprooted trees to the north of the airport boundary.

Charles Snider of the National Weather Service, Ann Arbor, Michigan. There was a downburst between Ann Arbor and Willow Run Airports where 75 and 57 mph peak gusts were measured, respectively. Wind effects increased from Detroit Metro Airport, where an 82 mph peak gust was recorded, toward the east causing the worst damage near the Detroit River.

The distribution of the peak gust wind speeds in Fig. 6 represents the values estimated by the authors on the basis of 22 anemometer measurements, including three 90 mph values, used as calibrations. Wind speeds above 100 mph (45 m s^{-1}) were estimated based on the comparison of damage from other survey cases where wind speeds were known; 151 mph at Tecumseh, Michigan airport, 115 mph at Rhinelander, Wisconsin airport, etc. In spite of the best-possible estimates by the authors based on calibrations and comparisons, the uppermost wind speeds in Fig. 6 may not be accurate with possible errors of 30 mph.

An interesting aspect of the Chicago-to-Detroit storms is the periodic occurrences of downburst clusters at ~70 min intervals. This periodicity is similar to that of family tornadoes known to occur at about 45 min intervals (e.g., Fujita, 1963).

4. Chicago area downburst cluster

Due to the lack of uniformly distributed trees in the Chicago area, it was not feasible to determine the exact number of downbursts. The worst damage occurred in the western suburbs where roofs of apartment buildings were blown away. In some areas, electric power was out for more than 10 days.

At the Underwriter's Laboratory, 30 km NNW of Downtown Chicago, a peak gust of 90 mph (40 m s^{-1}) occurred in a microburst which lasted for only 2 min (see Fig. 7). The microburst winds were superimposed upon the gust-front winds which had started 5 min earlier. A ground survey showed that tree and structural damage near the laboratory was minimal. Wind effects increased southward suggesting that there was a band of 100 mph or stronger winds extending to Lake Michigan (see Fig. 5).

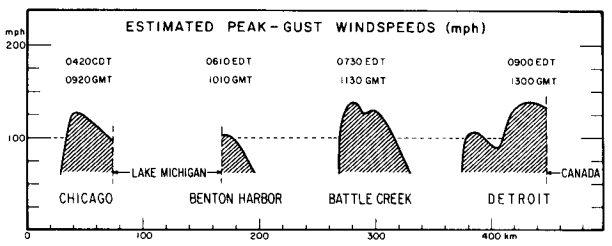

FIG. 6. Periodic occurrences of downburst clusters and their estimated peak-gust wind speeds. Estimates were made by Fujita (Chicago area), Fujita and Abbey (Battle Creek area), and Snider (Detroit area). These clusters occurred in ~70 min intervals.

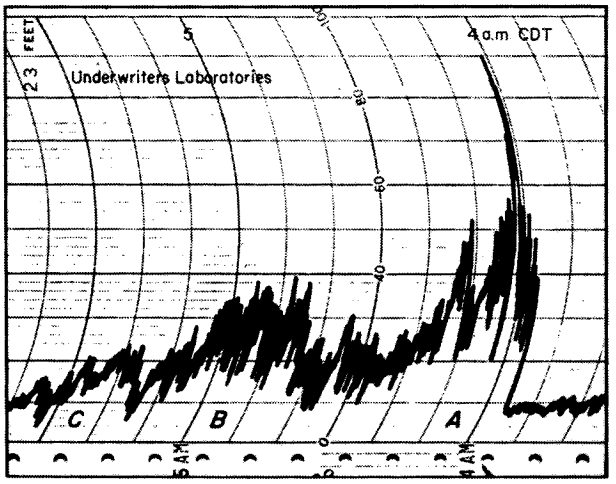

FIG. 7. A 90 mph (40 m s^{-1}) peak gust of a microburst which occurred 5 min after the passage of a gust front at 0356 CDT 16 July 1980. The microburst wind lasted for only 2 min. (Courtesy of Underwriter's Laboratory, Chicago).

A microburst to the southwest of The University of Chicago was surveyed in detail. The anemometer at The University recorded only a 61 mph peak gust, and the damage around the anemometer was limited to trees which had lost a few twigs and branches.

The wind effects increased significantly from the anemometer location toward the southwest. There was a narrow zone, 200–300 m wide, extending from Washington Park to Jackson Park in which trees were snapped and uprooted.

A comparison of the damage distribution in Fig. 8 and the anemometer record in Fig. 9 shows that the area around The University of Chicago was affected by the fringe of a microburst which moved from the northwest.

The barograph trace recorded at the anemometer site showed a significant pressure jump at the onset of the gust-front winds. No pressure nose, expected to occur near the center of a microburst, was recorded, because the barograph site was located near the fringe of the microburst (see Fig. 10).

Superimposed upon the gust-front winds was a microburst with an 800 m wide band of damaging winds. Since Fig. 9 shows a single peak gust of less than one minute, the dimension of the microburst in the direction of its movement was probably of the order of 1500 m if it moved at 25 m s^{-1}. The lifetime of the microburst would have been ~4 min.

The anemometer record also reveals the existence of weaker wind disturbances of longer periods shown with letters A, B and C. Each of these disturbances lasted 20–40 min and also is identifiable in the wind trace from the Underwriter's Laboratory in Fig. 7. The time differences are ~30 min indicating that these disturbances travelled through

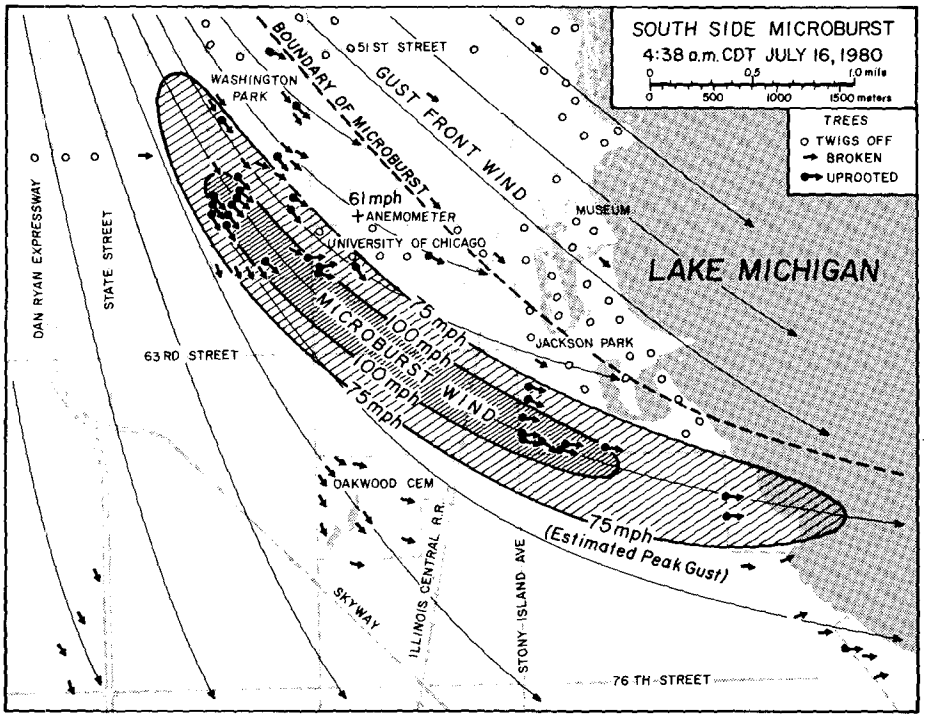

FIG. 8. A microburst near The University of Chicago, south side of Chicago. The estimated 75 mph (33 m s^{-1}) damage swath was 800 m wide and 6500 m long. This damage swath missed the anemometer at The University of Chicago by ~200 m. The microburst was accompanied by blinding rain.

a distance of 43 km in 30 min or at 86 km h^{-1} (54 mph).

The linear dimensions of the south side microburst in Fig. 8 present a problem in regard to the representativeness of winds recorded by most network stations. Network stations with 1 km spacing may or may not be located along the center axis of

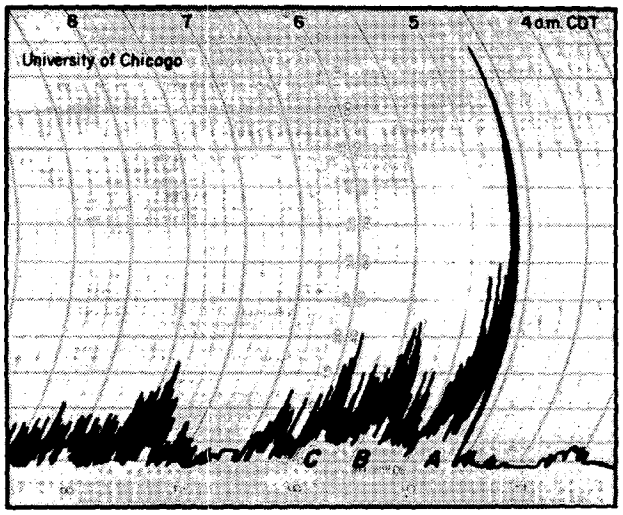

FIG. 9. Peak gust of 61 mph (27 m s^{-1}) recorded at The University of Chicago at 0438 CDT 16 July 1980. The anemometer was located near the outer edge of the microburst mapped in Fig. 8. Wind damage increased significantly toward the southwest where the estimated peak gust was in excess of 100 mph (45 m s^{-1}). (Courtesy of the Department of Geophysical Sciences.)

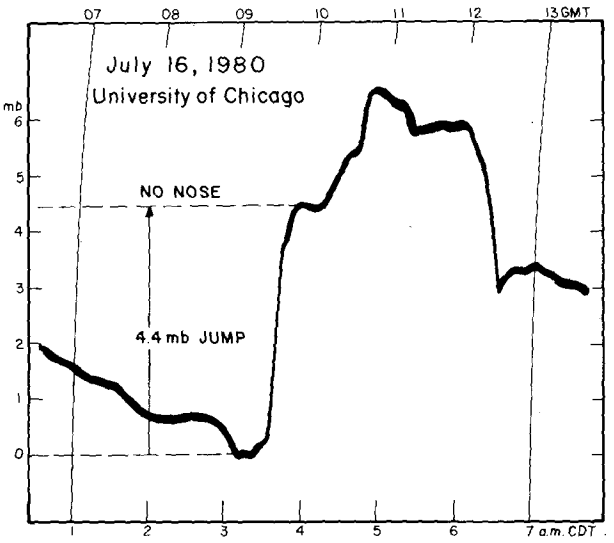

FIG. 10. Pressure trace recorded at the anemometer site of The University of Chicago. A 4.4 mb pressure jump occurred when the gust front passed. However, no pressure nose of the microburst in Fig. 8 was detected.

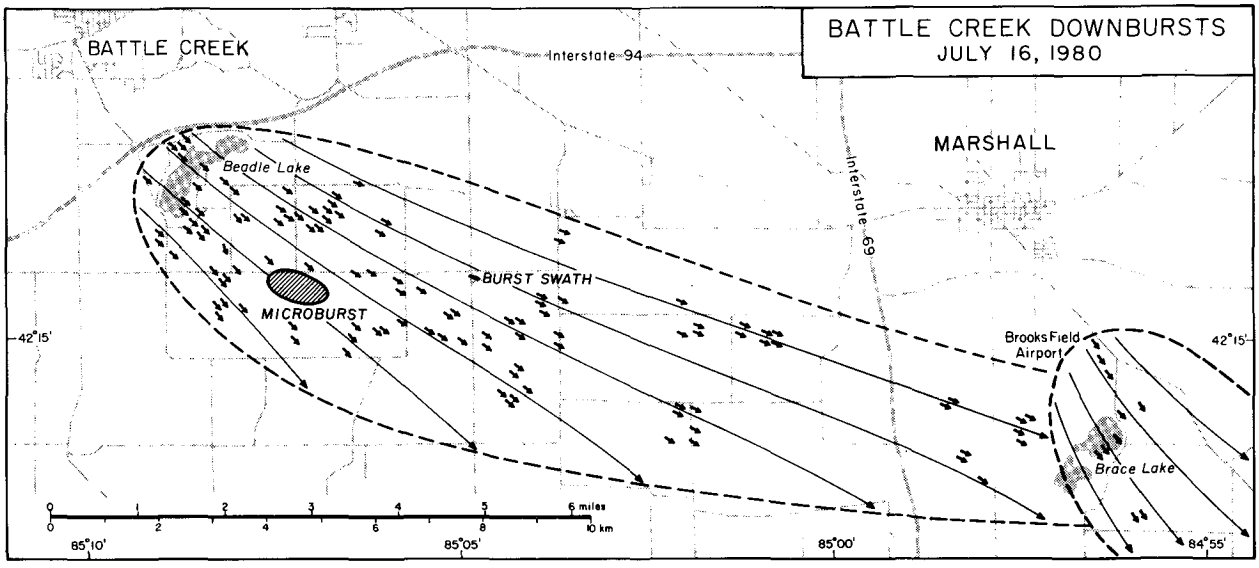

FIG. 11. Two Battle Creek downbursts, one originating to the southeast of the city, and the other to the south of Marshall. Arrows show the direction of uprooted trees. A microburst and burst swath are enlarged in Figs. 13 and 25.

this size of microburst. It would be necessary to distribute stations with 100–200 m spacing in order to map the wind field. Therefore, the chance of a single wind tower recording the maximum winds in a microburst appears to be remote.

5. Battle Creek downbursts

In response to a telephone call from Robert Jacobson (Lansing National Weather Service) aerial photography of the downbursts in the Battle Creek area was made by Wakimoto ~30 h after the storm. This downburst cluster, consisting of two major downbursts, occurred over a flat farming area. The wind effects in the wake of these downbursts provided us with the basic data for investigating the airflow characteristics of extreme winds.

Kellogg Airport, to the west of Battle Creek, measured a 75 mph peak gust as the city was affected by strong winds which broke twigs off trees. The damage along Interstate 94 was minimal.

However, a large number of trees to the west of Beadle Lake, less than one mile from the Interstate, were uprooted (see Fig. 11). The downburst damage continued to Brace Lake south of the city of Marshall. The directional divergence of this downburst was only 10–20°, suggesting that the storm moved relatively quickly toward the east-southeast.

The second downburst started to the south of Marshall where a 5.3 mb pressure jump followed by a 2.2 mb pressure nose was recorded (see Fig. 12). It is likely that the foot of a downdraft passed over Marshall shortly before the strong winds started to the south of the city.

The downflow speed giving rise to this pressure nose can be computed as

$$\left.\begin{aligned} \tfrac{1}{2}\rho w^2 = 2.2 \text{ mb}, \quad \rho = 1.2 \text{ kg m}^{-3} \\ w = 19 \text{ m s}^{-1} = 43 \text{ mph} \end{aligned}\right\}, \quad (1)$$

where w denotes the downflow speed above the barograph at Marshall. This pressure nose is comparable to that of a microburst in Florida studied in detail by Caracena and Maier.[6]

The wind effects in Marshall were relatively weak with no tree damage visible from the air. At the Marshall Fire Department the wind indicator went off the scale at 90 mph, the maximum scale of the instrument.

Similar reports of 90+ mph peak gusts were made by the Sheridan-Albion Fire Department and by the Hormer Environmental Station, both of which were located outside the boundary of the downburst area as determined by Wakimoto. It appears that uprooted trees are visible from the air when peak-gust speeds exceed 90–100 mph (40–45 m s^{-1}).

6. Airborne objects inside the first Battle Creek downburst

A microburst and a burst swath in the first downburst mapped in Fig. 11 were surveyed in detail. The microburst was located 3 km to the southeast of Beadle Lake, and the burst swath 3 km east of the microburst.

It is generally thought that high-density objects, such as bricks and blocks, can become airborne in tornadoes, but not in straight-line winds. Three

[6]Caracena, F., and M. Maier, 1979: Analysis of a microburst in the FACE meteorological mesonetwork. *Preprints Eleventh Conf. Severe Local Storms*, Kansas City, Amer. Meteor. Soc., 279–290.

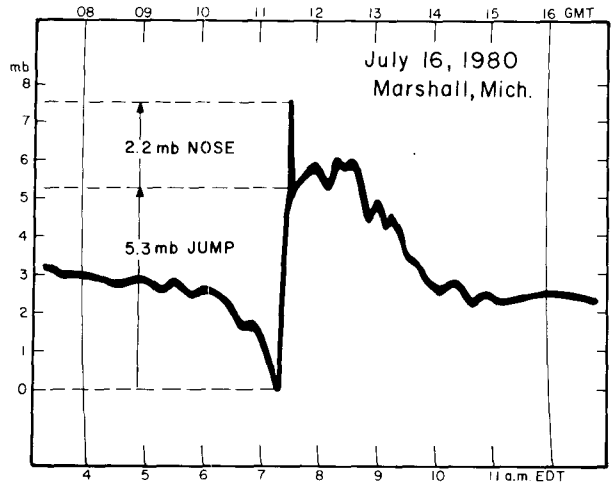

FIG. 12. Barograph trace recorded at Marshall, Michigan. A 5.3 mb pressure jump was followed by a 2.2 mb pressure nose (Courtesy of Mr. Bob Thompson.)

types of flying objects were found inside these local wind disturbances. They are (i) a 180 kg chimney which flew 105 m over a one-story house (in the burst swath); (ii) a 1000 kg corn storage bin which flew 163 m and then rolled 590 m (in the microburst); and (iii) 5 cm × 10 cm × 100 cm lumber blown into the cornfield, 90–170 m away (in the microburst).

The microburst in which (ii) and (iii) occurred was 1200 m long and 400 m wide, extending from the Aldrich Farm to a residential area to the east (Fig. 13).

There were three bins at the southeast corner of the farm. The eastern bin was ~10% full, the center bin was empty, and the western bin was under construction. The center bin L in Figs. 13–15 was picked up by the wind. It flew south for 163 m and hit a mulberry tree M in the field, receiving a dent at its top. Thereafter, it rolled in the cornfield leaving 34 V-notches along the 590 m roll mark. The distance between successive notches was 17.3 m.

The circumference of the bin, 5.5 m in diameter, is 17.2 m which turned out to be the distance between the V-notches. This coincidence implies that the bin had rolled in the field without a measurable slippage, being pushed by the microburst winds from the northwesterly direction. Slight changes in the roll direction were probably caused by the larger diameter of the top cover of the bin, by the deformation as it rolled down the field, and by the

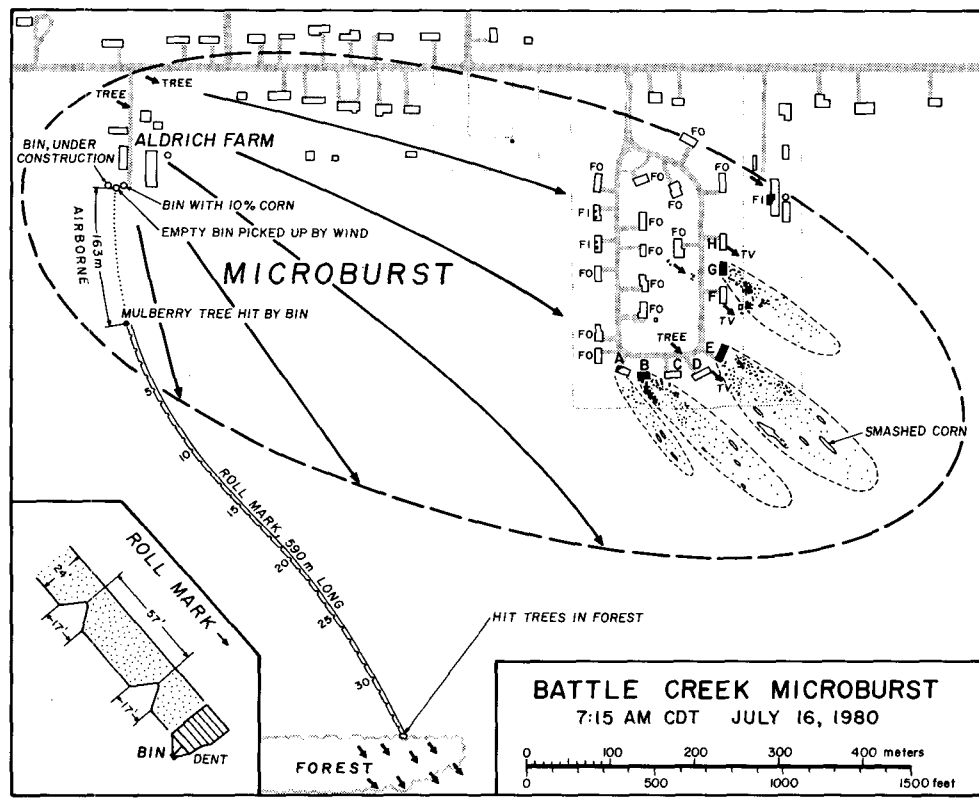

FIG. 13. Detailed map of a microburst in Fig. 11. An empty bin in the Aldrich Farm was picked up by the wind and a number of houses farther to the east were damaged.

irregular surface of the cornfield. We should not assume that the roll direction represents the instantaneous direction of the wind.

Twenty-three houses in the residential area were in the microburst. Two were under construction while the others were up to 10 years old. The lumber (iii) was blown off the roofs of several houses, smashing into the cornfield to the southeast (Fig. 13).

The chimney (i) had been attached to the roof which was blown away. Since it is very unlikely that the chimney alone became airborne, the roof and chimney must have flown together at least part of the way.

The foregoing findings indicate that various objects can fly inside a microburst or a burst swath. We shall review the response of objects exposed to high winds in an ultimate attempt to estimate the maximum wind speeds.

In general, the degree of damage becomes progressively worse as the wind speed increases. Expected wind effects are as follows:

[I] Elastic deformation—no change in shape after the wind

[II] Permanent deformation—object deforms permanently

[III] Vertical dislocation—object blown down

[IV] Horizontal dislocation—object blown away

Of these, [I] can be used for measuring the wind speed based on the deformation-wind-speed relationships. The measured values represent the wind speed averaged both in time and space, provided that the natural frequency of the deforming object is higher than the wind speed fluctuations. The measured wind speed decreases with the size of the object, because the larger the averaging area, the lower the mean wind speed.

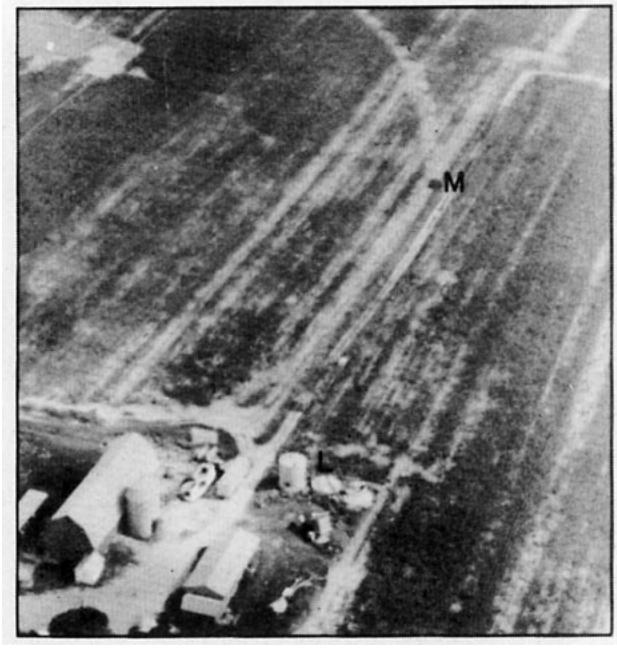

FIG. 14. View of the Aldrich Farm, looking south. The middle bin L was lifted off toward the south. After hitting a mulberry tree M in the field, the bin rolled 590 m. (Photo by Wakimoto on 17 July.)

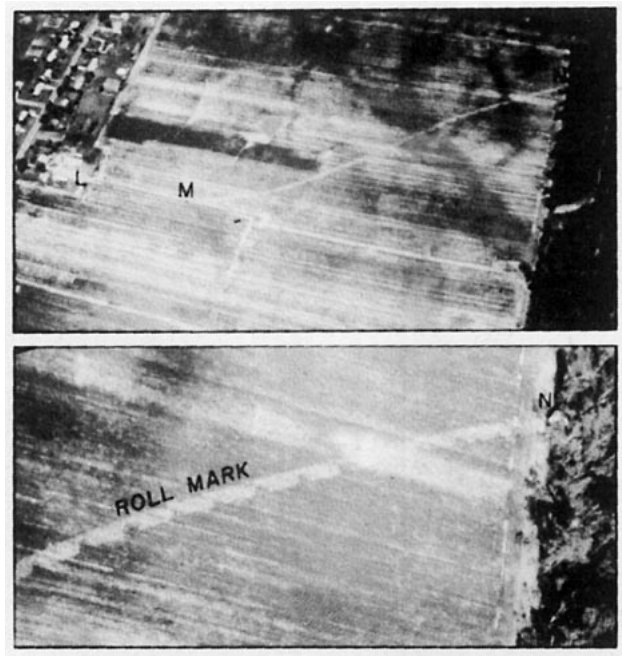

FIG. 15. The path of the bin from its origin L to the mulberry tree M to the final position N (above). An enlarged view of the roll mark with periodic "V notches" (below). (Photo by Wakimoto on 17 July.)

[II] and [III] are frequently used for estimating, not for measuring, the damage-causing wind speeds. For basic principles, assumptions and assessment results, refer to Minor *et al.* (1972).

It should be noted that the estimate error of the "maximum wind speed" increases from [II] to [III], because more assumptions and unknowns are involved as deformation is upgraded to dislocation.

We now consider the case in which a first (slower) peak wind is followed by a second (stronger) peak wind. An object initially deformed [II] by the first wind may or may not be further deformed by the second peak wind, as much as it would be deformed if the second wind came first.

When an object is blown down to the ground by the first peak wind [III] (vertical dislocation), the blown-down object resting on the ground is protected against the second peak wind due to the lower wind speed near the ground. In other words, the object does not always respond to the second stronger wind, resulting in the underestimation of the maximum wind speed.

The expected accuracy of the assessed maximum wind speeds based on blown-away objects [IV] is

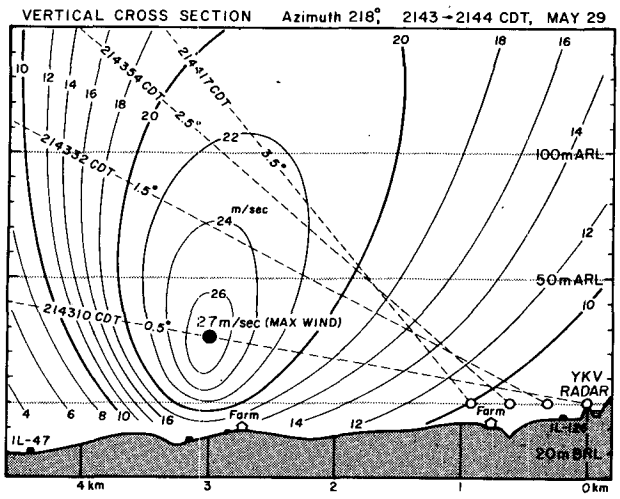

FIG. 16. Vertical cross section of the microburst winds of 29 May 1978 measured by NCAR's CP-3 Doppler radar during the Project NIMROD. Height scales are in meters above radar level (ARL) or below radar level (BRL).

worse because we have to make stringent assumptions regarding time and spatial variations of wind speeds, airborne mechanisms, modes of flight, and many others.

Mehta[7] indicated that calculations of wind speeds based on flying objects are in the questionable credence-level category. In other words, we must face the reality that the higher the wind speeds, the larger the estimate error.

In swaths of extreme wind, however, it is common to see dislocated objects [III] and [IV] rather than deformed objects [II]. Furthermore, ground and aerial surveys reveal that there is a greater prevalence of blown-away objects [IV] as the suspected maximum wind speeds increase. Even though wind speed estimates from blown-away objects are less accurate than those from damaged structures, in some cases data on blown-away objects are the only ones available; hence it is often worthwhile to estimate wind speeds from flying objects. The exclusion of speed estimates based on flying objects may seriously underestimate the maximum wind speed inside very small short-lived weather systems.

It is customary to express estimated wind speeds in integers, such as 103 mph or 89 m s^{-1}, giving an impression of 1 mph or 1 m s^{-1} accuracy. However, it is highly unlikely that the maximum wind speeds can be estimated with a 1 mph (0.5 m s^{-1}) accuracy, because the estimates involve assumptions of drag and lift coefficients, profiles and time variations of impinging winds, pre-wind strength of objects and structures, time sequences of structural failure in relation to wind-speed variations, and many more. In view of inevitable errors applicable to all estimates, a specific range of error should be accompanied by each estimated value, e.g., 172 ± 10 mph or 102 ± 10 m s^{-1}.

7. Estimates of wind speeds in microbursts and burst swaths

The foregoing documentation and discussion of airborne objects imply that the winds inside a downburst could be locally very high. How fast is the maximum wind speed? How high above the ground does it occur? These questions need to be answered.

During Project NIMROD (Northern Illinois Meteorological Research On Downburst), on 29 May 1978, outburst winds in an approaching microburst were scanned by a Doppler radar from 2 to 4 km distance, obtaining a 27 m s^{-1} maximum wind speed located only 30–40 m above the ground. This finding implies that the maximum outburst winds could be located just above the top of tall structures (Fig. 16).

Wind-speed estimates based on blown-away objects [IV] include large inevitable error. Nevertheless, we must attempt to make estimates because the opportunity of measuring the missile generating wind speeds in microbursts by Doppler radar will be rare, if not nil.

a. Ballistic trajectory

The simplest flight mode of an airborne object is the ballistic trajectory expressed by

$$X = V_0 t, \quad H = V_0 t \tan\theta - \tfrac{1}{2} g t^2, \tag{2}$$

where X and H are, respectively, the horizontal distance and the height of a ballistic object at time t. The elevation angle of the initial velocity is expressed by θ, and the gravitational acceleration by g (Fig. 17).

If the ballistic object lands where $H = 0$ and $X = X_0$, we obtain the airborne time

$$t_0 = \left(\frac{2 X_0 \tan\theta}{g}\right)^{1/2} \tag{3}$$

and the ballistic horizontal speed

$$V_0 = \left(\frac{g X_0}{2 \tan\theta}\right)^{1/2} \tag{4}$$

which remains constant during the entire ballistic flight.

Numerical values of t_0 and V_0 in Table 2 computed from Eqs. (3) and (4) reveal that the airborne time is only less than 10 s within the ranges of the airborne distance of up to 250 m, and the elevation angle up to 60°.

[7]Mehta, K. C., 1976: Wind speed estimates: Engineering analyses. *Proc. Symposium on Tornadoes,* Institute for Disaster Research, Texas Tech University, Lubbock, 89–102.

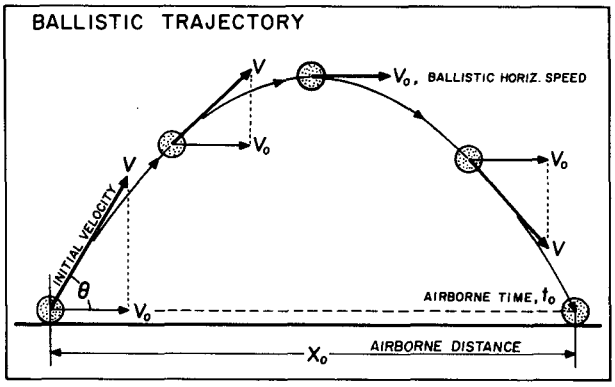

FIG. 17. A ballistic trajectory characterized by the elevation angle θ of the initial velocity, the ballistic horizontal velocity V_0 and the airborne distance X_0. V_0 remains constant during the airborne time t_0.

b. *Non-ballistic, wind-accelerated flight*

An object which becomes airborne in high winds does not gain its initial velocity instantaneously. Instead, it is accelerated by both lift and drag forces provided by the impinging wind W. The vertical forces acting upon the object after the break off can be expressed by

$$\text{Vertical force} = \tfrac{1}{2} C_L A_H \rho W^2 - Mg, \qquad (5)$$

where C_L is the lift coefficent, A_H the horizontal cross-sectional area of the object, ρ the density of the air and M the mass of the object (Fig. 18).

The horizontal force, likewise, is given by

$$\text{Horizontal force} = \tfrac{1}{2} C_D A_V \rho W^2, \qquad (6)$$

where C_D is the drag force and A_V the vertical cross-sectional area of the object perpendicular to the wind.

The horizontal speed V_H of the object being accelerated by the horizontal force in Eq. (6) can be written as

$$V_H = W\left[1 - \left(1 + \frac{W t}{B_0}\right)^{-1}\right], \qquad (7)$$

which approaches W, the speed of the impinging wind as time t increases. The quantity B_0, to be called the ballistic length, is defined by

$$B_0 = \frac{2}{C_D}\frac{\rho_0}{\rho} L_0, \qquad (8)$$

where ρ_0 is the density of the object and L_0 the characteristic length of the object computed from

$$L_0 = \frac{\text{Volume of object}}{\text{Vertical cross sectional area of object}}$$

which varies with the orientation of the object relative to the impinging wind.

TABLE 2. Airborne time t_0 (s) and horizontal speed V_0 (m s^{-1}) of a ballistic missile computed as functions of airborne distance X_0 (m) and elevation angle θ (deg) of the initial velocity.

Elevation angle θ	Airborne distance X_0									
	50 m		100 m		150 m		200 m		250 m	
	t_0	V_0	t_0	V_0	t_0	V_0	t_0	V_0	t_0	V_0
10°	1.3	37	1.9	53	2.3	65	2.7	75	3.0	83
20°	1.9	26	2.0	37	3.3	45	3.9	52	4.3	58
30°	2.4	41	3.4	29	4.2	36	4.9	41	5.4	46
45°	3.2	16	4.5	22	5.5	27	6.4	31	7.1	35
60°	4.2	12	6.0	17	7.3	21	8.4	24	9.4	27

c. *Estimate of wind speeds*

A combination of the ballistic and non-ballistic flights presented herein can be used in estimating wind speeds in microbursts. Assumptions for the estimate are as follows:

(i) Object becomes detached a moment before the arrival of the peak, horizontal wind.

(ii) The peak wind is vertically uniform, maintaining its speed during the entire airborne time of several seconds.

(iii) The deviation of the object trajectory from the corresponding ballistic trajectory is assumed small, so that the airborne time of the object can be computed from Eq. (3) as a function of X_0 and θ.

The airborne distance X_0 can be measured accurately through a post-storm survey. We must, however, estimate θ based on both liftoff and landing conditions of each airborne object.

Since the object hits the ground at X_0 at time t_0, the horizontal speed in Eq. (7) must satisfy the condition

$$X_0 = \int_0^{t_0} V_H \, dt \qquad (9)$$

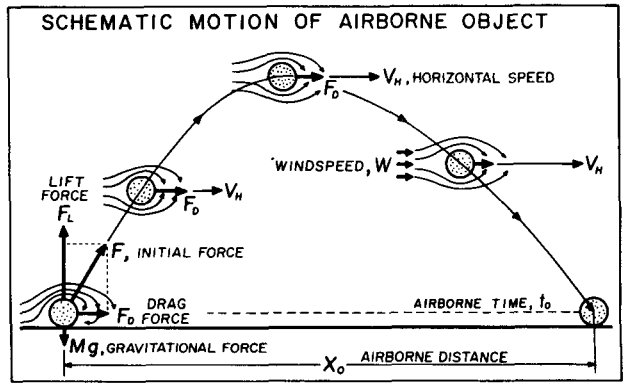

FIG. 18. Schematic trajectory of an airborne object accelerated by lift and drag forces. V_H, the horizontal speed of the object approaches W, the impinging wind speed as time increases.

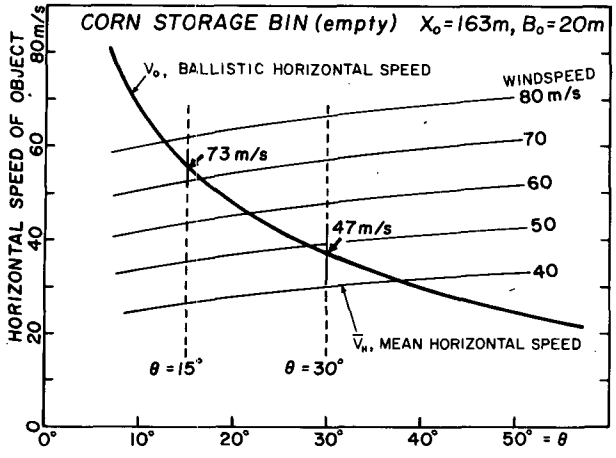

FIG. 19. Horizontal speed versus elevation angle diagram (speed-angle diagram) for estimating the wind speed required to fly the corn storage bin at the Aldrich Farm. Semi-horizontal isotachs labeled with five wind speeds denote the mean horizontal speeds of the bin induced by the labeled wind speeds.

which is now integrated into

$$X_0 = W t_0 - B_0 \ln\left(1 + \frac{W t_0}{B_0}\right). \qquad (10)$$

Dividing both sides of this equation by t_0, we obtain the mean horizontal speed of the object averaged over the entire airborne distance X_0 which is

$$\overline{V}_H = W - \frac{B_0}{t_0} \ln\left(1 + \frac{W t_0}{B_0}\right). \qquad (11)$$

This equation will permit us to compute the mean horizontal speed of the object as a function of X_0 and θ, because t_0 in Eq. (3) includes both X_0 and θ.

This means that a group of isopleths of $\overline{V}_H$ for a given airborne distance and ballistic length can be drawn on a horizontal speed vs elevation angle diagram, abbreviated as the "speed-angle diagram," which is to be used in estimating wind speed with a specified range of estimate error.

d. *Wind speed in microburst estimated from airborne storage bin*

The technical data of the corn storage bin (empty) which flew away from the Aldrich Farm are

Diameter of bin	5.5 m (18 ft)
Height of bin	7.3 m (24 ft)
Volume of bin	173 m^3
Mass of bin only	800 kg
bin with air inside	1000 kg
Density of bin only	7.9 kg m^{-3}
bin with air inside	5.8 kg m^{-3}
Ballistic length of bin with air	20 m
Drag coefficient	2.0 (assumed)
Airborne distance	163 m
Estimated elevation angle	15–30°

The base of this bin had been tied down to a circular concrete foundation with small 2.5 mm bolts and nuts. They were, apparently, sheared off prior to the onset of the peak wind.

The mean horizontal speeds of the bin under five different impinging wind speeds are shown in a speed-angle diagram (Fig. 19). The diagram also includes a curve of V_0, computed from Eq. (4) by changing θ between 10° and 60°. The intersections of five isotachs and V_0 curve indicate that a 47 m s^{-1} wind speed is required if the bin had flown with θ = 30°. When θ is reduced to 15°, the required wind speed increases to 73 m s^{-1}.

Ground inspection revealed that the mulberry tree, in the direct path of the bin was bent, but not crushed. The descending angle of the bin estimated from the height of the tree and the location of the first roll mark behind the tree is 15–30°.

The wind speeds estimated from the speed-angle diagram (Fig. 19) of this airborne bin are between 47 and 73 m s^{-1}, which may be expressed by 60 ± 13 m s^{-1} (135 ± 30 mph).

e. *Wind speed in microburst estimated from blown-away lumber*

Eight houses to the east of the Aldrich Farm were in the microburst wind. Table 3 shows the characteristics of these houses identified as A–H.

An aerial view of these houses (Fig. 20) reveals that a large number of boards from the damaged houses were blown toward the southeast into the cornfield. The damage was caused by straight-line winds of the microburst. No tornado was involved (Fig. 2A1).

House E (Fig. 21) is single-story structure with an extended roof. It lost all of the roofing tiles and 40% of the roofing boards. 5 cm × 10 cm lumber and insulation materials were blown into the corn-

TABLE 3. Characteristics of houses A–H in the residential area.

Houses	Stories	Years old	Damage by microburst winds
A	1	3	20% of roof tiles peeled off
B	Near completion		Whole structure blown down
C	1	5	No damage to house; antenna blown down
D	2	8	No damage to house; antenna blown down
E	1	10	Lost 100% roof tiles and 40% roof boards
F	1	4	No damage to house; antenna blown down
G	Under construction		Whole structure blown off foundation
H	1	5 to 10	No damage to roof; tall antenna blown down

FIG. 20. An aerial view of houses A–H in Fig. 13. Pieces of the roofs were blown into the cornfield, smashing the cornstalks which were about 4 ft tall. Houses B and G were under construction.

field, 90–170 m away. Ground inspection showed that the impact angles of these objects were very shallow, implying that they smashed into the cornfield with descending angles of 15 to 25° (Fig. 22).

The technical data of the blown-away lumber for the wind speed estimate are

Dimensions of lumber	0.05 m × 0.1 m × 1 m
Volume of lumber	0.05 m^3
Mass of lumber	3.5 kg
Density of lumber	700 kg m^{-3}

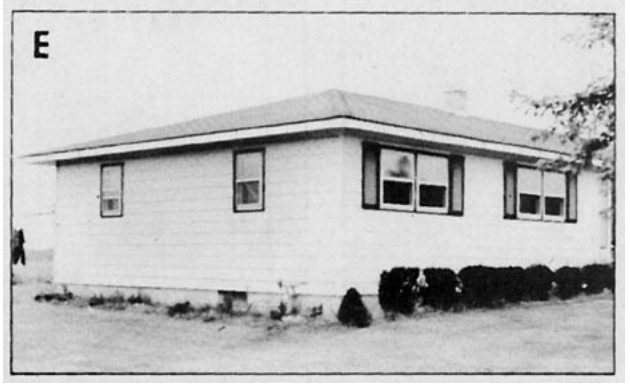

FIG. 21. A 10-year-old house E which lost most of its roof (repaired). (Photo, looking south, by Fujita and Abbey on 6 August.)

FIG. 22. Pieces of the roof from house E blown into cornfield. Corn had grown from 4–7 ft after the damage on 16 July. (Photo by Fujita and Abbey on 6 August.)

Ballistic length	30 m (shortest)
Drag coefficient	2.0 (assumed)
Airborne distance	150 m
Estimated elevation angle	15–25°

The shortest ballistic length used in this estimate will produce the maximum acceleration of the lumber. However, a piece of lumber changes its orientation during the flight, thus varying its ballistic length from 30 m with impinging wind on its broad side, to 60 m on the narrow side, to 600 m in the longitudinal direction. Since lumber is likely to tumble in the wind, the use of B_0 = 30 m will result in an underestimate of the wind speed.

The initial height of the lumber on the roof was ~3 m above the cornfield. This height will extend the airborne distance by 6–11 m. In view of this

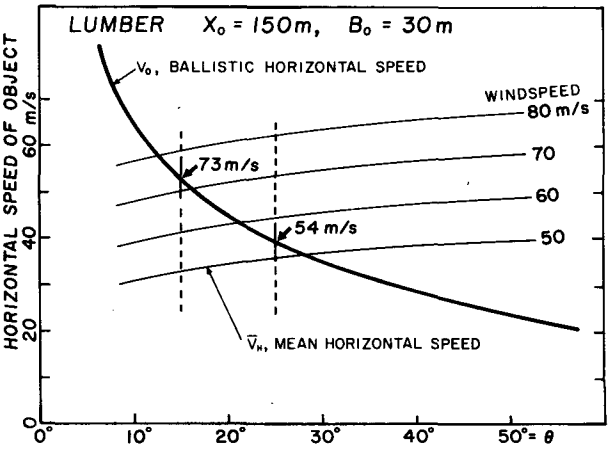

FIG. 23. Speed-angle diagram for estimating the wind speed required to fly the lumber in Fig. 22.

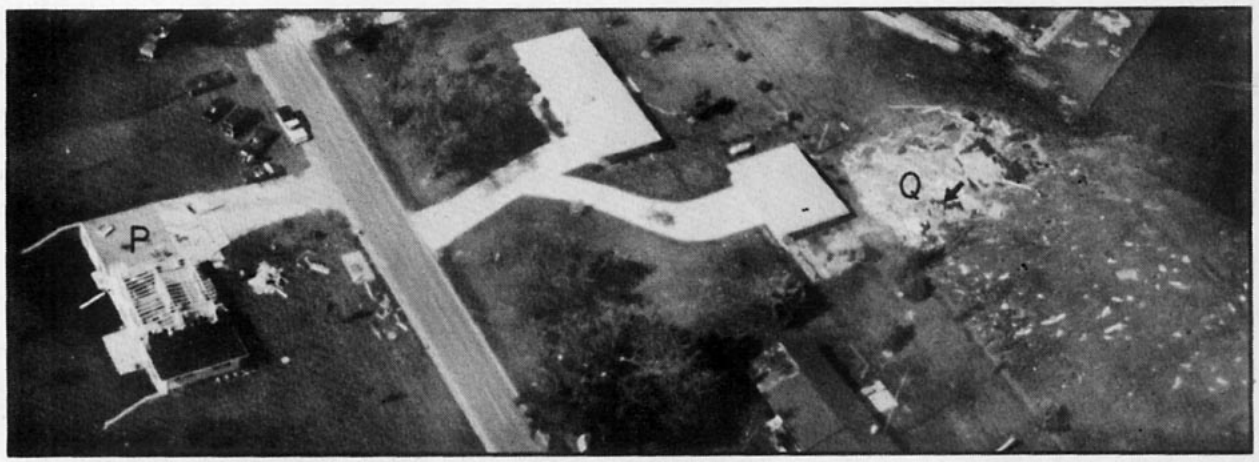

FIG. 24. Aerial view of an unroofed house P and its roof landed upside down at Q. Apparently, the roof flew clear over a house and descended in a steep angle on the east side of the house. An arrow denotes the location of a 390 lb (180 kg) chimney.

elevation difference, the airborne distance of 150 m was used, instead of 170 m, the maximum airborne distance measured.

The wind speeds estimated from the speed-angle diagram (Fig. 23) of the blown-away lumber are between 54 and 73 m s^{-1} (120 and 160 mph) or 63 ± 10 m s^{-1} (140 ± 20 mph). The total airborne time estimated is between 2.9 and 3.8 s, indicating that the flight of lumber requires <4 s of the peak wind.

f. Wind speeds in burst swath estimated from airborne chimney

About 3 km to the east of the microburst, a house was unroofed by a localized high wind. Its roof flew away toward the east-southeast passing over a house on the other side of a highway and landed upside down in a grass field (Fig. 24).

Detailed mapping of the unroofed house and vicinity revealed the existence of a burst swath across the house. The direction of the debris from the upside-down roof was divergent as much as 90° (Fig. 25), giving an impression that the winds close to the ground diverged from the wreckage area (Fig. 2A4).

A close inspection of the damage resulted in the finding of a 180 kg (390 lb) chimney inside the wreckage of the roof. The chimney was 43 cm square and 86 cm tall (Fig. 26). The airborne distance of the chimney was 105 m.

Aerial photographs and ground inspection of the wreckage of the roof indicated that the descent angle of the roof which cleared the house must be at least 20°. Meanwhile the maximum descent angle, estimated from the debris scatter in a 20 m × 30 m area, turned out to be up to 35°. A hypothetical

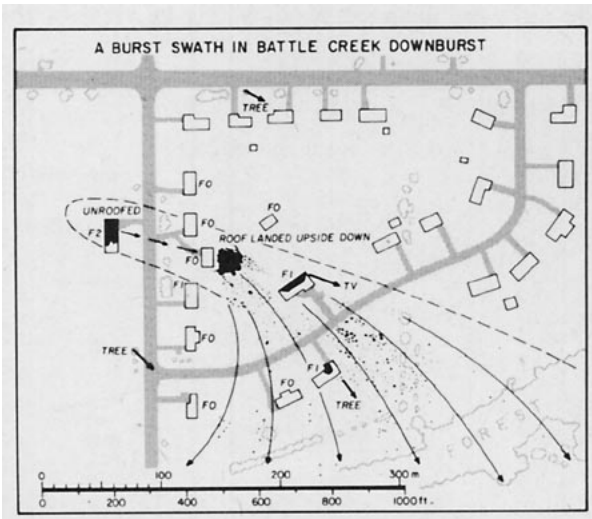

FIG. 25. Damage map of the area around the houses in Fig. 24. The width of the burst swath, extending toward the east-southeast, was only ~50 m.

FIG. 26. A close-up view of the 390 lb (180 kg) chimney consisting of 66 bricks, each weighing 5 lb (2.3 kg). (Photo by Fujita and Abbey on 6 August.)

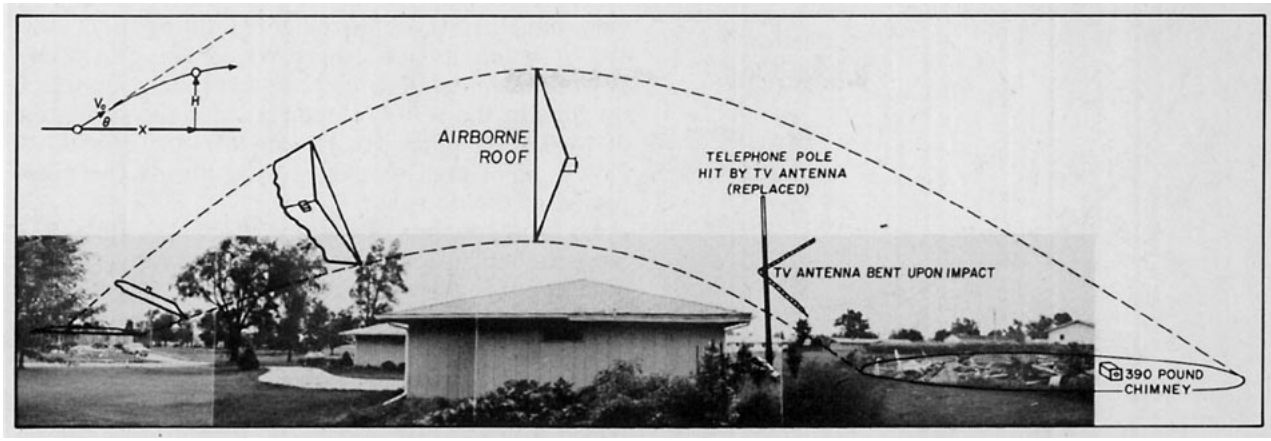

FIG. 27. Estimated path of the airborne roof which could have been thrown upward in a 30–45° angle. A 390 lb (180 kg) chimney was found in the broken-up roof, 105 m from its origin. (Photo by Fujita and Abbey on 6 August.)

trajectory of the roof, thus constructed, is shown in Fig. 27.

The technical data for estimating the wind speeds based on this airborne chimney are:

Dimensions of chimney	0.43 m × 0.43 m × 0.86 m
Dimensions of roof	0.025 m × 9 m × 15 m
Volume of chimney	0.159 m^3
Volume of roof	3.375 m^3
Mass of chimney	180 kg
Mass of roof	2430 kg
Density of chimney	1130 kg m^{-3} (with air inside)
Density of roof	700 kg
Ballistic length of chimney	400 m (with air inside)
Ballistic length of roof	15 m
Drag coefficient	2.0 (assumed)
Airborne distance	105 m
Estimated elevation angle	20–35°

The airborne time computed from Eq. (3) is between 2.8 and 3.9 s which results in the ballistic horizontal speed ranging between 38 and 27 m s^{-1}. A speed-angle diagram (Fig. 28) of the airborne chimney shows that the range of the wind speeds is between 93 and 130 m s^{-1}, if the chimney flew independent of the roof.

By attaching 100% of the roof, the ballistic length of the roof/chimney system decreases to only 16 m. The isotachs of wind speeds on the right side of the speed-angle diagram reveals that the range of the wind speeds required is 36 to 51 m s^{-1}, a significant decrease.

Table 4 was prepared to show the variation of the estimated wind speeds as a function of the percent of the roof attached to the chimney. An attachment of only 10% of the roof reduces the maximum wind speed from 130 to 55 m s^{-1}.

To find the chimney inside the roof wreckage suggests that the ballistic lengths of the chimney with roof and the roof alone must be close to each other. Otherwise the segment of the roof, free from the chimney, must be found further away from the

TABLE 4. Estimated wind speeds of the airborne chimney computed by changing the percent of the roof which flew with the chimney.

		Chimney with percent of the roof				
	Chimney only	10%	20%	30%	100%	Roof only
Mass (kg)	180	423	666	909	2610	2430
Volume (m^3)	0.159	0.497	0.834	1.172	3.534	3.375
Density (kg m^{-3})	1132	851	799	775	739	700
Ballistic length (m)	400	25	21	18	16	15
		Estimated wind speeds				
$\theta = 20°$	130	55	53	52	51	50 m s^{-1}
	290	123	119	116	114	112 mph
$\theta = 35°$	93	40	38	37	36	36 m s^{-1}
	208	89	85	83	81	81 mph

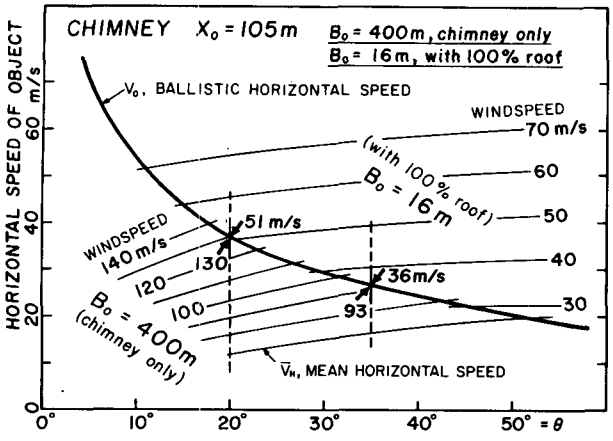

FIG. 28. Speed-angle diagram for estimating the windspeeds required to fly the chimney with or without the roof. 93–130 m s^{-1} (208–290 mph) wind speed is required to fly the chimney alone, while only 36–51 m s^{-1} (81–114 mph) is needed, with 100% of the roof attached.

chimney. The flight of the chimney with 10–100% of the roof will permit the landing of both chimney and roof inside a relatively small, confined area.

The maximum wind speeds satisfying above conditions are 36 to 55 m s^{-1} (114 to 123 mph) or 45 ± 10 m s^{-1} (101 ± 24 mph).

8. Cloud-top temperature depicted by enhanced infrared imagery

The life of the downburst family between Chicago and Detroit on 16 July was about 5.5 h between 0830 and 1400 GMT. Enhanced IR imagery, however, revealed that the area enclosed by the −60°C isotherm formed near Winona, Minnesota at 0400 GMT and lasted until 1600 GMT, a period ~12 h.

The −60°C or colder area increased rapidly, reaching a peak value at 0900 GMT, shortly after the onset of the first downburst cluster. Thereafter the area was more or less constant until it began shrinking rapidly after the end of the Detroit downbursts.

The most significant feature atop the parent cloud is the formation of a large warm area in the south-central region of an oval-shaped cloud (see Fig. 29). The warm area started as a V-shaped wake at 0830 GMT. Then the wake enlarged into a U-shaped warm area at 0900 and 0930 GMT. Finally the warm area reached its peak size at 1000 GMT shortly after the Chicago downbursts.

The overshooting activities depicted by the areas enclosed by the −66°C isotherms diminished rapidly after the formation of the Chicago downbursts (see Fig. 30).

These features of the enhanced cloud tops are very similar to those documented during the 4 July 1977 downbursts in northern Wisconsin. The intensity of the downbursts increased to their peak when the area of the −70°C clouds reached the minimum at 1400 GMT (Fig. 31). Meanwhile, the growth of −59°C anvil area shrunk slightly during the peak period of the downbursts.

So far the events of 16 July 1980 and 4 July 1977 were the most significant downburst days well-documented through aerial mapping of the damage. In these two cases overshooting areas decreased significantly during intense downbursts, giving a false impression that the nephsystem was decaying. Instead, it signaled the onset of the strong downbursts which caused heavy damage beneath the shrinking areas of the cold cloud tops.

9. Conclusions

Damaging winds induced by thunderstorms have been classified into tornado and straight-line winds. Tornadoes have been well-documented by virtue of their appearance and devastating wind effects. Straight-line winds, on the other hand, are loosely defined, often giving an impression of gusty winds behind a gust front.

Meso- and miso-scale analysis of the 16 July 1980 storms suggests a need for the subclassification of straight-line winds into two categories, downburst and gust-front.

Although downburst winds are generally weaker than tornado winds, the probability of their occurrence at a given location is much higher than that of tornadoes. For example, the total dollar damage of the 16 July 1980 downbursts in Michigan, Illinois, Wisconsin and Minnesota was approximately $650 million, because the storm affected large areas in four states.

Infrared imagery of geostationary satellites began showing definite cloud-top signatures associated with large and strong downbursts on the ground. It will also be feasible to detect downburst-producing echoes by using advanced future radars.

In order to undertake downburst forecasting in future years, it is necessary to 1) establish enhancement and pattern recognition techniques of satellite imagery, 2) improve detection and display capabilities of future radars, 3) confirm and report downbursts to improve national statistics, and 4) perform theoretical and numerical studies of downburst phenomena.

Acknowledgments. The authors wish to express their appreciation to Messrs. Neil J. Levine and Michael B. Duval and Ms. Roberta F. Ellis, research staff of the Satellite and Mesometeorology

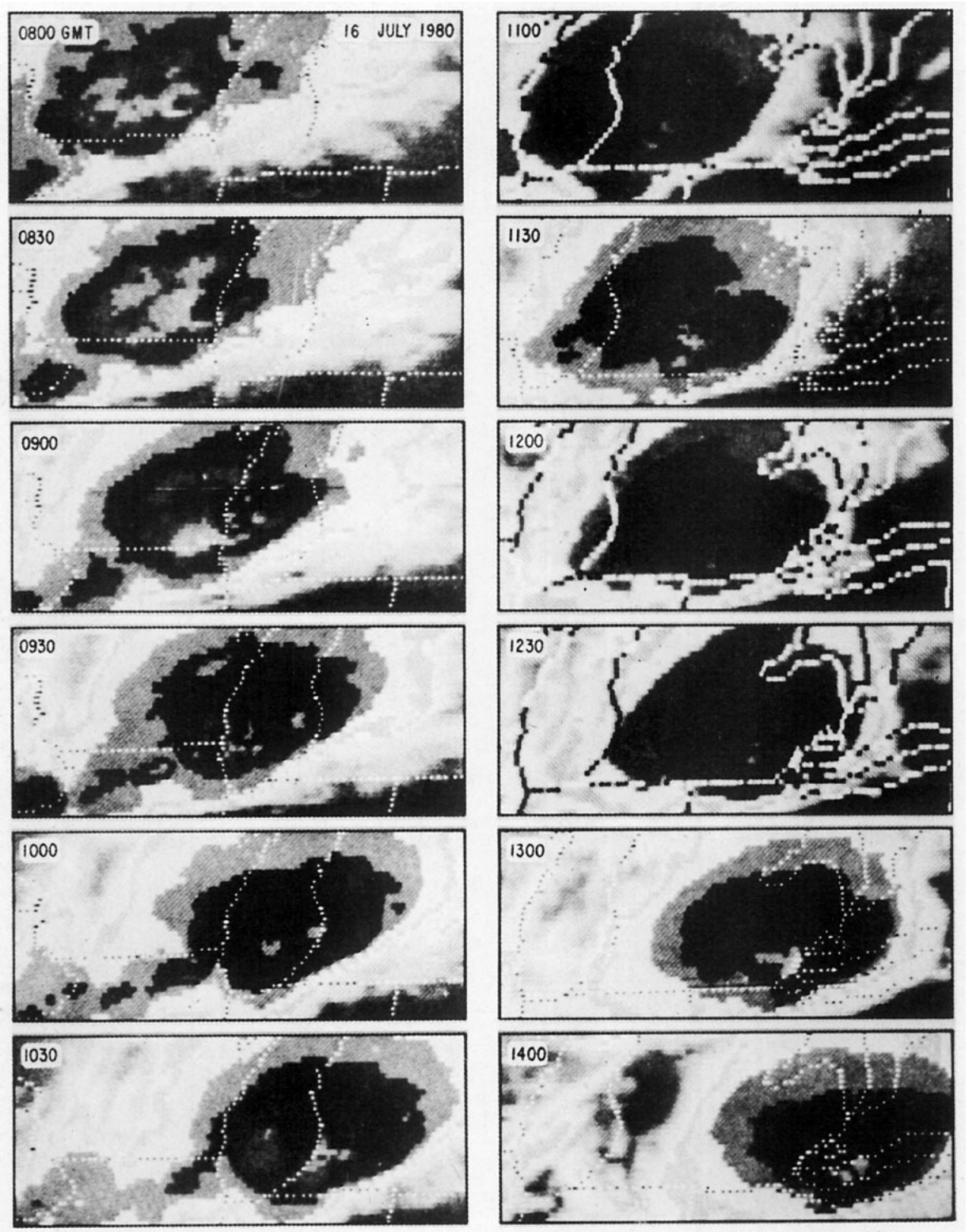

FIG. 29. A series of enhanced (Mb curve) IR imagery showing −60°C anvil areas in black. Overshooting areas within the anvil are shown with graduated gray. The coldest cloud tops warmed up significantly between 0900 and 0930 GMT when downbursts began in the Chicago area.

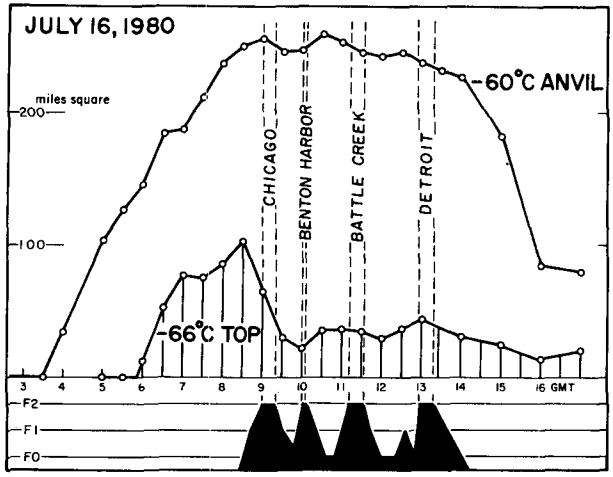

FIG. 30. Variation of cloud-top areas defined by −60 and −66°C isotherms of enhanced IR imagery. Areas are expressed by the units of miles square. Overshooting areas depicted by −66°C isotherms increased rapidly until 0830 GMT when Chicago downbursts started. Then the areas remained small during the Chicago to Detroit downbursts.

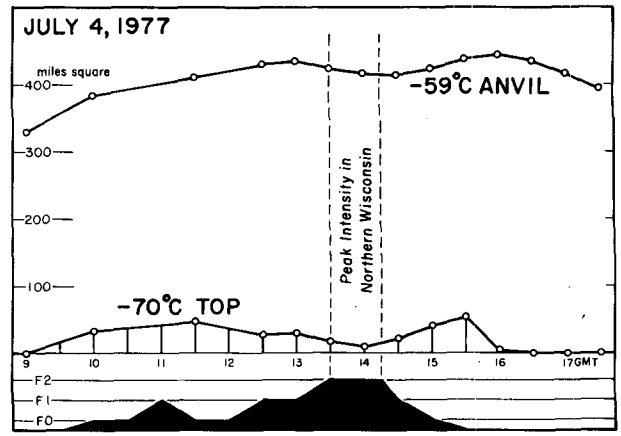

FIG. 31. A similar decrease in the overshooting areas was evidenced during the Northern Wisconsin downburst, one of the worst non-tornadic storms in the area.

Research Project, for their effort in surveying the 16 July 1980 storms.

Vital data for storm survey and analysis were supplied by the National Weather Service Offices at Lansing, Ann Arbor, Detroit and Chicago, as well as the National Environmental Satellite Service at Kansas City and Washington, DC. The personal cooperation of Messrs. Robert Jacobson, Charles Snider, Raymond Waldman, Edward Ferguson, Linwood Whitney and Frederick Ostby is highly appreciated.

Ground survey of the Battle Creek downbursts, leading to the wind speed estimates, was performed with Mr. Robert Abbey of the Nuclear Regulatory Commission.

Meteorological results reported in this paper have been sponsored by NOAA under Grant NA80AA-D-00001, by NASA under Contract NGR 14-001-008, and by NSF under Grant NSF/ATM 79-21260. Wind speed estimates have been supported by NRC under Contract NRC 04-74-239.

REFERENCES

Byers, H. R., and R. R. Braham, 1949: *The Thunderstorm*. U.S. Govt. Printing Office, Washington, DC, 287 pp.

Fujita, T. T., 1963: Analytical mesometeorology: a review. *Meteor. Monogr.*, No. 27, Amer. Meteor. Soc.,, 77–128.

——, 1973: Tornadoes around the world. *Weatherwise*, **26**, 56–62, 78–83.

——, D. L. Bradbury and C. F. Van Thullenar, 1970: Palm Sunday tornadoes of April 11, 1965. *Mon. Wea. Rev.*, **98**, 29–69.

——, and H. R. Byers, 1977: Spearhead echo and downburst in the crash of an airliner. *Mon. Wea. Rev.*, **105**, 129–146.

——, and F. Caracena, 1977: An analysis of three weather-related aircraft accidents. *Bull. Amer. Meteor. Soc.*, **58**, 1164–1181.

Fujiwara, S., 1943: Report of special observation of thunderstorms. Japan Meteor. Agency, 248 pp.

Koschmieder, H., 1955: *Ergebnisse der Deutschen Böenmessungen 1939/41*. Friedr. Vieweg & Sohn, Braunschweig, 148 pp.

Minor, J. E., K. C. Mehta and J. R. McDonald, 1972: Failures of structures due to extreme winds. *J. Structural Div. ASCE*, **98**, 2455–2471.

Müldner, W., 1950: Die Windbruchschäden des 22.7.1948 im Reichswald bei Nürenberg. *Berichte Dtsch. Wetterdienstes* (U.S. Zone), **19**, 3–39.

Suckstorff, G. A., 1938: Kaltlufterzeugung dürch Niederschlag. *Z. Meteor.*, **55**, 287–292.